Am J Cancer Res 2023;13(11):5320-5333
www.ajcr.us /ISSN:2156-6976/ajcr0152848

Original Article

Silencing of m^{6}A methyltransferase KIAA1429 suppresses the progression of non-small cell lung cancer by promoting the p53 signaling pathway and ferroptosis

Yuanzhou Wu, Hui Li, Yang Huang, Qunqing Chen

Department of Thoracic Surgery, Zhujiang Hospital, Southern Medical University, Guangzhou 510280, Guangdong, China

Received August 9, 2023; Accepted November 1, 2023; Epub November 15, 2023; Published November 30, 2023

Abstract: KIAA1429, an important component of the N6-methyladenine methyltransferase complex, is involved in the pathology of many types of cancer. In this study, the mechanisms through which KIAA1429 promotes non-small cell lung cancer (NSCLC) progression were explored using *in vitro* and *in vivo* experiments. Additionally, bioinformatics analysis of publicly available data was used to determine the relationship between KIAA1429 expression and NSCLC patient survival. The results showed that KIAA1429 was upregulated in NSCLC tissues and cells, and its high expression level was associated with low overall survival. Transcriptome analysis of *KIAA1429*-silenced NSCLC cells identified 346 differentially expressed genes, which were enriched in ferroptosis and the p53 signaling pathway. *KIAA1429* silencing using small interfering (si) RNA promoted erastin-induced ferroptosis in NSCLC cells and activated the p53 signaling pathway. Moreover, si-KIAA1429 inhibited the proliferative, migratory, and invasive abilities of NSCLC cells *in vitro* and tumor growth *in vivo.* These *in vitro* effects were weakened by pifithrin-μ, a p53 inhibitor. Therefore, given its effects on ferroptosis and the p53 signaling pathway, targeting KIAA1429 could be an effective strategy for treating NSCLC.

Keywords: Non-small cell lung cancer, KIAA1429, ferroptosis, N6-methyladenine, p53 signaling pathway

Introduction

Non-small cell lung cancer (NSCLC) is a common form of lung cancer, the three main subtypes of which are adenocarcinoma, squamous cell carcinoma, and large-cell carcinoma [1]. As a malignant tumor with a high incidence and mortality rate, NSCLC is a serious threat to human health [2]. Clinically, the treatment of NSCLC depends mainly on a combination of surgery and adjuvant chemotherapy [3]. Although tyrosine kinase inhibitors and immunotherapy have improved the survival of NSCLC patients [3, 4], the overall cure and survival rates remain unsatisfactory, particularly in patients with metastases [5]. Nonetheless, an increasing number of molecular targets with therapeutic potential against NSCLC have been discovered, providing additional possibilities for improving patient outcomes [6, 7].

The transcriptional modification of eukaryotic mRNAs is important for ensuring the proper splicing, editing, stability, and degradation of gene transcripts. The most commonly occurring post-transcriptional modification is the methylation of the sixth nitrogen atom of adenine, otherwise known as N6-methyladenine (m^{6}A), which is carried out by a methyltransferase complex [8]. Functionally, mRNAs with m^{6}A participate in various pathophysiological processes, including adipogenesis, cell differentiation, proliferation, and apoptosis, and immune and inflammatory responses [9]. Notably, m^{6}A-modified mRNAs are involved in the development of lung cancer [10]. Evidence has demonstrated that diverse m^{6}A-related factors can regulate the malignant behavior of NSCLC cells by acting as oncogenes (e.g., *ALKBH5*) or anti-oncogenes (e.g., *FTO*, *METTL3*, *HNRNPA2B1*, and *YTHDF1*) [11]. Among the main components of the meth-

yltransferase complex, KIAA1429 (also known as protein virilizer homolog (VIRMA)) is the largest methyltransferase involved in m^{6}A methylation [12]. KIAA1429 plays a key regulatory role in the tumorigenesis and progression of liver [12], breast [13], gastric [14], and colorectal cancers [15]. Additionally, KIAA1429-mediated m^{6}A modification promotes the progression of NSCLC and accelerates the resistance of the cancer cells to gefitinib [16, 17]. However, the mechanism of action of KIAA1429 in NSCLC remains unclear.

Ferroptosis, which is a specific type of iron-related programmed cell death, is involved in various human diseases, including ischemia-reperfusion injury, degenerative diseases, cardiovascular diseases, and several types of cancer [18, 19]. Many potential molecular targets are involved in the progression of NSCLC through their regulation of ferroptosis, including SLC7A11 [20], MT1DP [21], AKR1C1 [22], miR-302a-3p [23], and circDTL [24]. Ferroptosis can also be mediated by m^{6}A modification [25, 26]. Song et al. showed that miR-4443 enhanced cisplatin resistance in NSCLC by regulating FSP1 in an m^{6}A-like manner [27]. Additionally, the p53 signaling pathway, which is a crucial regulator of NSCLC, participates in the regulation of ferroptosis [28, 29].

In this study, we explored the mechanisms downstream of KIAA1429 in NSCLC using transcriptome sequencing. We found that differentially expressed genes (DEGs) in *KIAA1429*-silenced NSCLC cells were highly enriched in the p53 signaling pathway and ferroptosis process. Therefore, we used *in vivo* and *in vitro* experiments to further explore the potential mechanism by which KIAA1429 regulates ferroptosis and the p53 signaling pathway in NSCLC.

Materials and methods

Bioinformatics data analysis

KIAA1429 expression in 59 normal and 515 lung adenocarcinoma (LUAD) tissues was analyzed using The University of ALabama at Birmingham CANcer data analysis Portal (UALCAN, https://ualcan.path.uab.edu/index.html) based on The Cancer Genome Atlas database. The correlation between the KIAA1429 expression level and the survival prognosis of 239 patients with NSCLC was analyzed using the Gene Expression Profiling Interactive Analysis portal (http://gepia.cancer-pku.cn/). Additionally, datasets related to "lung cancer" were searched on the Gene Expression Omnibus database (https://www.ncbi.nlm.nih.gov/geo/) to verify the expression of KIAA1429 in human lung cancer and normal tissues. The microarray dataset GSE18842 was selected, and the expression of KIAA1429 was analyzed using Oncomine (https://www.oncomine.org/).

Cell culture and transfection

BEAS-2B (a normal human lung epithelial cell line) and A549 and H1299 (two human NSCLC cell lines) were purchased from the American Type Culture Collection (Manassas, VA, USA). The NSCLC cells were cultured in Dulbecco's modified Eagle's medium (DMEM), supplemented with 10% fetal bovine serum (FBS), 100 U/mL penicillin, and 100 mg/mL streptomycin, at 37°C under 5% CO_2. The BEAS-2B cells were cultured in RPMI-1640 medium and supplemented with the same components at 37°C under 5% CO_2.

Small-interfering RNAs (siRNAs) targeting *KIAA1429* (si-KIAA1429-1, -2, and -3) and the corresponding negative control (si-NC) were purchased from RiboBio (Guangzhou, China) and transfected into the NSCLC cells using Lipofectamine 3000 for 48 h. Additionally, H1299 and A549 cells were treated with the p53 inhibitor pifithrin-μ (PFT, 10 μM), the ferroptosis activator erastin (10 μM), or the ferroptosis inhibitor ferrostatin-1 (Fer-1, 2 μM) for 48 h. The siRNA sequences are listed in Table S1.

Quantitative reverse transcription-polymerase chain reaction

Total RNA was extracted from the NSCLC cells using TRIzol reagent (Thermo Fisher Scientific, Waltham, MA, USA) and reverse transcribed into cDNA. The quantitative reverse transcription-polymerase chain reaction (RT-qPCR) was performed on a 7300PLUS instrument (Applied Biosystems, Foster City, CA, USA) using the SYBR Green qPCR Kit (Thermo Fisher Scientific). The reaction procedure was as follows: pre-denaturation at 95°C for 10 min, followed by 36 cycles of denaturation at 95°C for 10 s and annealing at 60°C for 30 s. The relative mRNA expression level of *KIAA1429* was calcu-

lated using the $2^{-\Delta\Delta Ct}$ method with glyceraldehyde-3-phosphate dehydrogenase (*GAPDH*) as the internal control. The primer sequences are listed in Table S2.

Cell counting kit-8 assay

Cell viability was measured using the Cell Counting Kit-8 (CCK8) assay (Solarbio, Beijing, China). In brief, transfected NSCLC cells (2×10^4 cells/well) were seeded into a 96-well plate and cultured at 37°C for 24, 48, and 72 h. Subsequently, the cells were incubated with 10 μL of CCK8 reagent for 2 h. Finally, to determine the optimal value, the optical density (OD) at 450 nm was recorded every 1 h using a microplate reader (Multiskan SkyHigh, Thermo Fisher Scientific).

EdU staining

The Click-iT™ Plus EdU Cell Proliferation Kit (Thermo Fisher Scientific) was used to detect the proliferation of the NSCLC cells. In brief, the transfected cells (1×10^5 cells/well) were seeded into 24-well plates. After 2 h of incubation with 50 μM EdU reagent, the cells were first fixed with paraformaldehyde (4%) and then incubated with Triton X-100 (0.5%). Subsequently, the cells were incubated with the Click-iT Cocktail (Alexa Fluor 555; Thermo Fisher Scientific) for 30 min, followed by 4',6-diamidino-2-phenylindole solution for 10 min in the dark. The stained cells were photographed under a fluorescence microscope (BX53; Olympus, Tokyo, Japan).

Wound-healing assay

A wound-healing assay was performed to measure cell migration. In brief, transfected cells were first cultured to 90% confluency, and a wound gap was then created on the cell layer using a pipette tip. After wash with phosphate-buffered saline to remove cell debris, the cells were cultured for 24 h. The wound gap was photographed and measured under a microscope (Olympus) at 0 and 24 h post-wounding.

Transwell assay

Transwell chambers (Corning, Kennebunk, ME, USA) were used to conduct the transwell assay for detecting cell invasion. In brief, the transwell chamber was coated with Matrigel (BD, Franklin Lakes, NJ, USA), after which 2×10^4 transfected cells were seeded into the upper chamber and DMEM containing 20% FBS was added to the lower chamber. After 24 h, the cells in the lower chamber were fixed with paraformaldehyde (4%) and stained with crystal violet (0.5%). The stained cells were photographed under a microscope (Olympus).

Enzyme-linked immunosorbent assay

The cell culture supernatants were collected for measurement of their malondialdehyde (MDA), iron ion (Fe^{2+}), glutathione peroxidase (GSH), and reactive oxygen species (ROS) levels using enzyme-linked immunosorbent assay kits (Esebio, Shanghai, China). In brief, 50 μL of diluted sample was added to each well of a 96-well plate, followed by 100 μL of horseradish peroxidase (HRP)-labeled antibody, and the samples were incubated for 60 min at 37°C. Within 15 min after incubation, the OD value at 450 nm was measured using a microplate reader.

Transcriptome sequencing

H1299 cells transfected with either si-KIAA1429 or si-NC were used for transcriptome sequencing. In brief, mRNA was purified from the total RNA (poly(A) selection) isolated from the cells and randomly fragmented into 200-300 bp pieces using metal ion-catalyzed hydrolysis. Subsequently, a cDNA library was constructed and sequenced on an Illumina NovaSeq 6000 platform. After sequencing, the DEGs were analyzed using DESeq2. Gene Ontology (GO) and Kyoto Encyclopedia of Genes and Genomes (KEGG) pathway analyses were performed using the Database for Annotation, Visualization, and Integrated Discovery (http://david.abcc.ncifcrf.gov/).

Tumor formation in a mouse model

Female BALB/c nude mice (age: 4-5 weeks; Antaik, Beijing, China) were used to establish a xenograft tumor model (n = 6). H1299 cells (1×10^6) that had been stably transfected with KIAA1429-shRNA (LV-shKIAA1429) or NC-shRNA (LV-shNC) were subcutaneously injected into the right dorsal flank of the mice. The tumor volume was measured every 7 days. After 28 days, the mice were anesthetized with an intraperitoneal injection of pentobarbital

sodium (50 mg/kg) and euthanized by cervical dislocation. The excised tumor xenografts were weighed and then used to detect KIAA1429 protein expression. The animal experiments were approved by the local ethics committee and conducted in accordance with the Guide for the Care and Use of Laboratory Animals.

Hematoxylin-eosin staining

Fresh tissues were fixed with paraformaldehyde (4%) and embedded in paraffin, after which the paraffin block was sectioned into thin slices. The dried tissue sections were immersed sequentially in xylene and gradient ethanol solutions. Subsequently, the slices were stained with hematoxylin and eosin and then dehydrated using an ethanol gradient. Finally, the slices were sealed with neutral balsam and examined and photographed under an inverted biological microscope.

Immunohistochemistry

The paraffin-embedded tissue sections were dewaxed and rehydrated, and ethylenediaminetetraacetic acid was then added for antigen retrieval. Subsequently, hydrogen peroxide (3%) was added to inactivate endogenous peroxidase at ambient temperature. The slices were incubated with anti-Ki67 antibody (ab-15580; Abcam, Cambridge, MA, USA) at 4°C overnight, followed by HRP-labeled secondary antibody at 37°C for 1 h. Finally, the slices were stained with 3,3'-diaminobenzidine and hematoxylin and photographed under a microscope.

Western blot assay

Cells or tissues were lysed in radioimmunoprecipitation assay buffer to extract their total proteins, which were then separated using 10% sodium dodecyl sulfate-polyacrylamide gel electrophoresis and transferred onto a polyvinylidene fluoride membrane (Millipore, Danvers, MA, USA). The membrane was blocked with nonfat milk and incubated with primary antibodies raised against KIAA1429, prostaglandin-endoperoxide synthase 2 (PTGS2), phospholipid hydroperoxide glutathione peroxidase (GPX4), ferritin heavy chain (FTH1), protein p53, phosphorylated p53 (p-p53), and β-actin (all 1:1000 dilutions; Abcam) for 12 h. Subsequently, the membrane was incubated with HRP-conjugated IgG secondary antibody (Abcam) for 2 h. The protein bands were visualized using enhanced chemiluminescence, after which they were quantified using a Gel-Pro analyzer (Media Cybernetics, Rockville, MD, USA).

Statistical analysis

All data are presented as the mean ± standard deviation and were processed using Prism 7.0 (GraphPad, San Diego, CA, USA). The *t*-test was used for comparisons between two groups, whereas one-way analysis of variance and Tukey's test were used for comparisons among multiple groups. A *P*-value of < 0.05 was regarded as statistically significant.

Results

KIAA1429 is upregulated in NSCLC

The expression levels of KIAA1429 in the 59 normal and 515 LUAD tissue samples were analyzed using UALCAN and were significantly higher in the cancerous tissues than in the normal controls ($P < 0.01$; **Figure 1A**). Survival analysis using GEPIA revealed that the overall survival period of patients with low KIAA1429 expression levels was significantly longer than that of patients with high KIAA1429 expression levels ($P = 0.022$; **Figure 1B**), demonstrating that high KIAA1429 expression is related to a poor prognosis. Analysis of the GSE18842 dataset, which contains 46 lung cancer and 45 normal tissue samples, revealed that KIAA1429 was substantially higher in the cancerous samples (**Figure 1C**). Additionally, KIAA1429 was significantly more highly expressed in the H1299 and A549 cells than in the BEAS-2B cells ($P < 0.01$; **Figure 1D**).

Knockdown of KIAA1429 inhibits the proliferative, migratory, and invasive abilities of NSCLC cells

To explore the role of KIAA1429 in NSCLC, *KIAA1429* expression was silenced in the two NSCLC cell lines. The transfection of si-KIAA1429-1, -2, and -3 into H1299 and A549 cells was verified using RT-qPCR, and si-KIAA1429-3 was used for the subsequent experiments because it had the highest silencing efficiency of the three siRNAs ($P < 0.01$; **Figure 2A**). The viability of the si-KIAA1429-transfected H1299 and A549 cells was signifi-

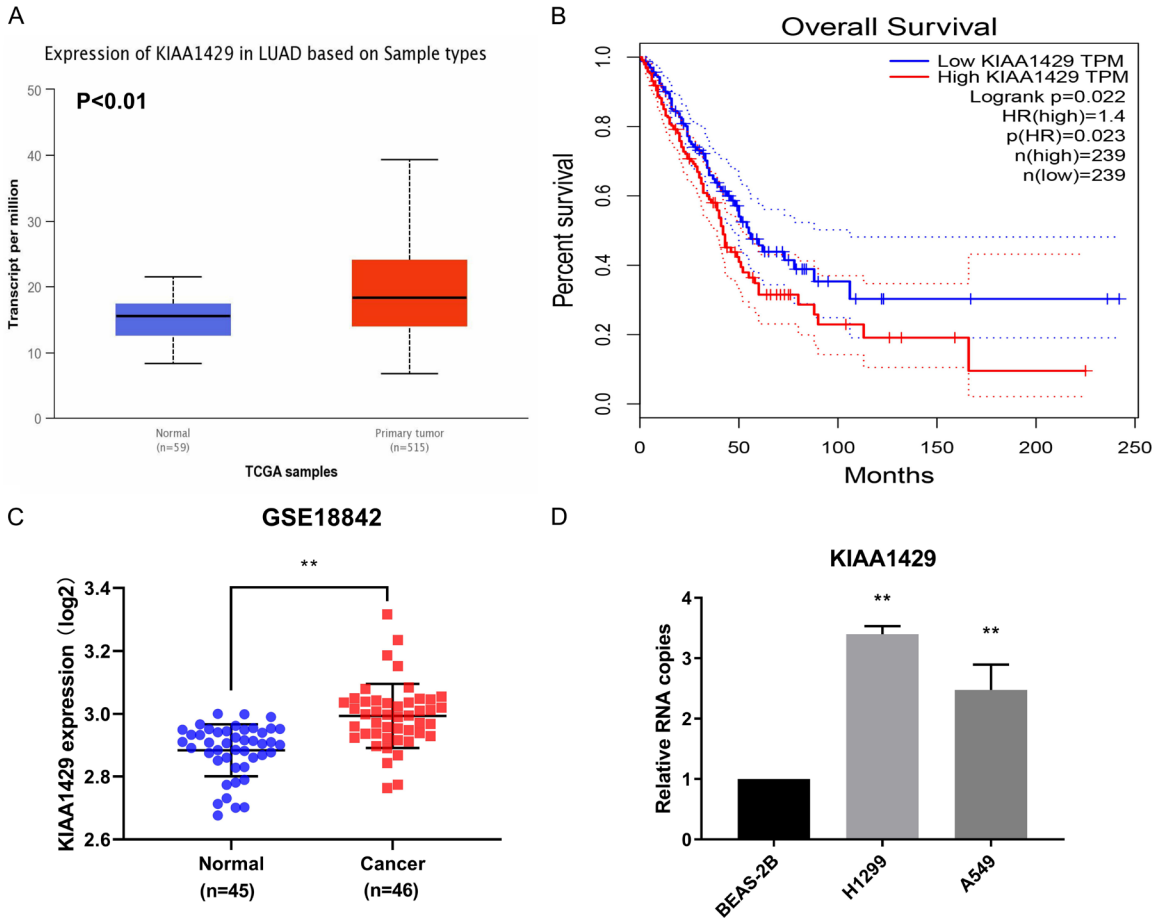

Figure 1. The up-regulation of KIAA1429 in NSCLC. A. The expression of KIAA1429 in LUAD tissues was analyzed using the UALCAN database. B. The correlation of KIAA1429 expression with overall survival in patients with LUAD was analyzed using GEPIA database. C. Oncomine was applied to evaluate KIAA1429 expression between cancer and normal tissues in microarray dataset (GSE18842). D. The expression of KIAA1429 in NSCLC cell lines (H1299 and A549 cells) and a normal lung epithelial cell line (BEAS-2B cells) was measured by qRT-PCR. **P < 0.01 vs. BEAS-2B.

cantly lower than that of the si-NC-transfected cells (P < 0.01; **Figure 2B**). Under the microscope, a lower EdU positivity rate was observed in the si-KIAA1429 groups than in the si-NC groups (P < 0.01; **Figure 2C**). Additionally, we found that si-KIAA1429 also inhibited the migratory and invasive abilities of the H1299 and A549 cells (P < 0.01; **Figure 2D** and **2E**).

Knockdown of KIAA1429 inhibits tumor growth in mice

To determine the role of KIAA1429 in NSCLC *in vivo*, H1299 cells transfected with either NC-shRNA or KIAA1429-shRNA were injected into mice. The tumor volume was lower in the LV-shKIAA1429 group than in the LV-shNC group on the 14th day post-inoculation (P < 0.05; **Figure 3A** and **3B**). The LV-shKIAA1429 group also had significantly low tumor weights on the 28th day post-inoculation (P < 0.01; **Figure 3C**). The western blotting results verified the downregulation of KIAA1429 expression in the tumor tissues of mice in the LV-shKIAA1429 group (P < 0.01; **Figure 3D**). Moreover, the knockdown of *KIAA1429* significantly reduced the degree of tumor malignancy (**Figure 3E**) and decreased the proliferation of the cancer cells (**Figure 3F**).

Knockdown of KIAA1429 promotes ferroptosis in NSCLC

si-KIAA1429 significantly reduced the viability of the erastin-treated NSCLC cells (H1299 and A549), and the inhibitory effect was greater

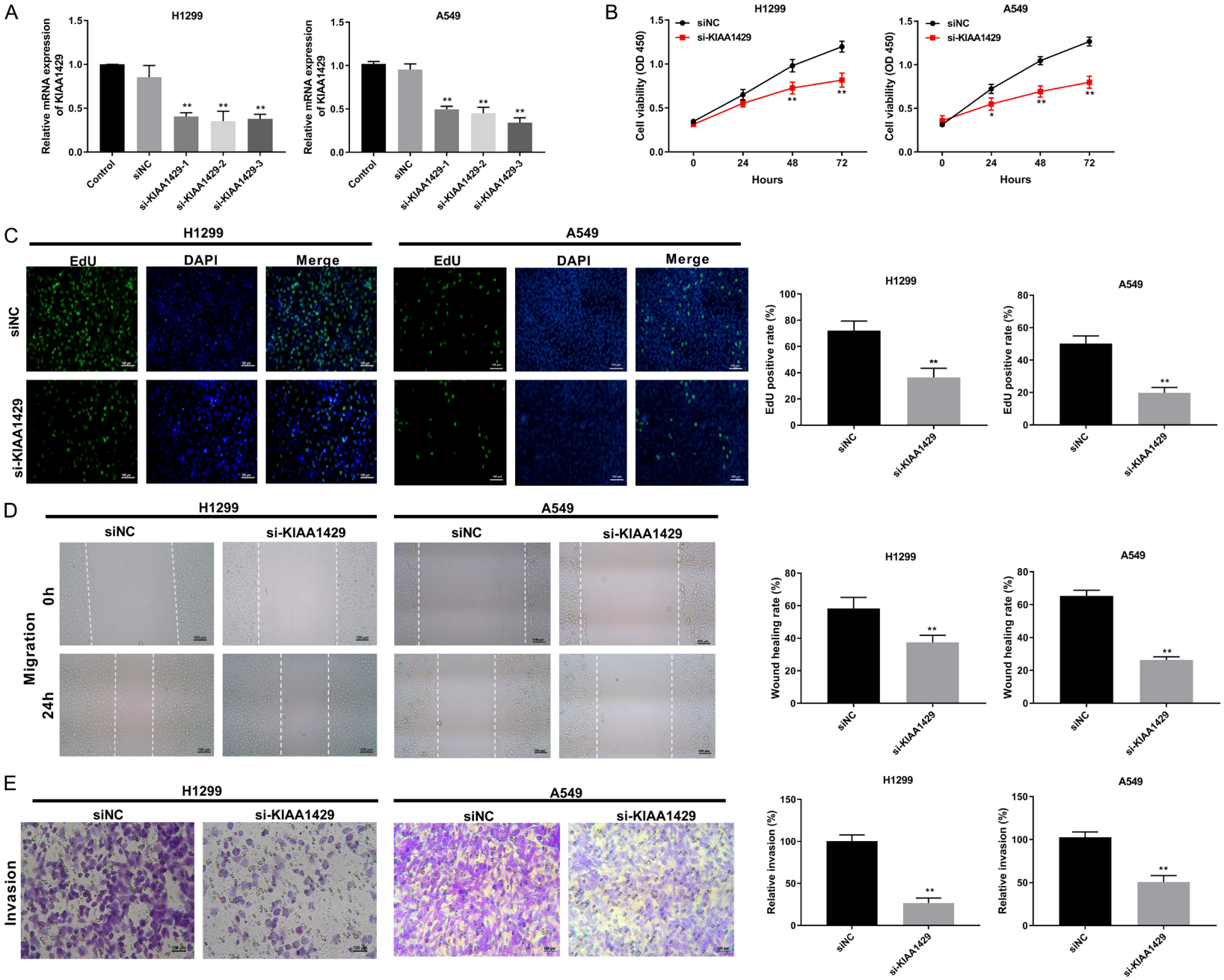
A
H1299
A549
Relative mRNA expression of KIAA1429
Control
siNC
si-KIAA1429-1
si-KIAA1429-2
si-KIAA1429-3
B
H1299
A549
siNC
si-KIAA1429
Cell viability (OD 450)
Hours
C
H1299
A549
EdU
DAPI
Merge
siNC
si-KIAA1429
EdU positive rate (%)
D
H1299
A549
siNC
si-KIAA1429
Migration
0h
24h
Wound healing rate (%)
E
H1299
A549
siNC
si-KIAA1429
Invasion
Relative invasion (%)

Figure 2. Knockdown of KIAA1429 inhibited the proliferation, migration, and invasion of NSCLC cells. A. The expression level of KIAA1429 in NSCLC cells transfected with si-KIAA1429-1/-2-/-3/si-NC was detected by qRT-PCR. B. The viability of transfected NSCLC cells was measured by CCK8 assay. C. EdU positive cells were detected by EdU assay (200×). D. The migration of transfected NSCLC cells was measured by wound healing assay. E. The invasion of transfected NSCLC cells was measured by Transwell assay (200×). *P < 0.05, **P < 0.01 vs. siNC.

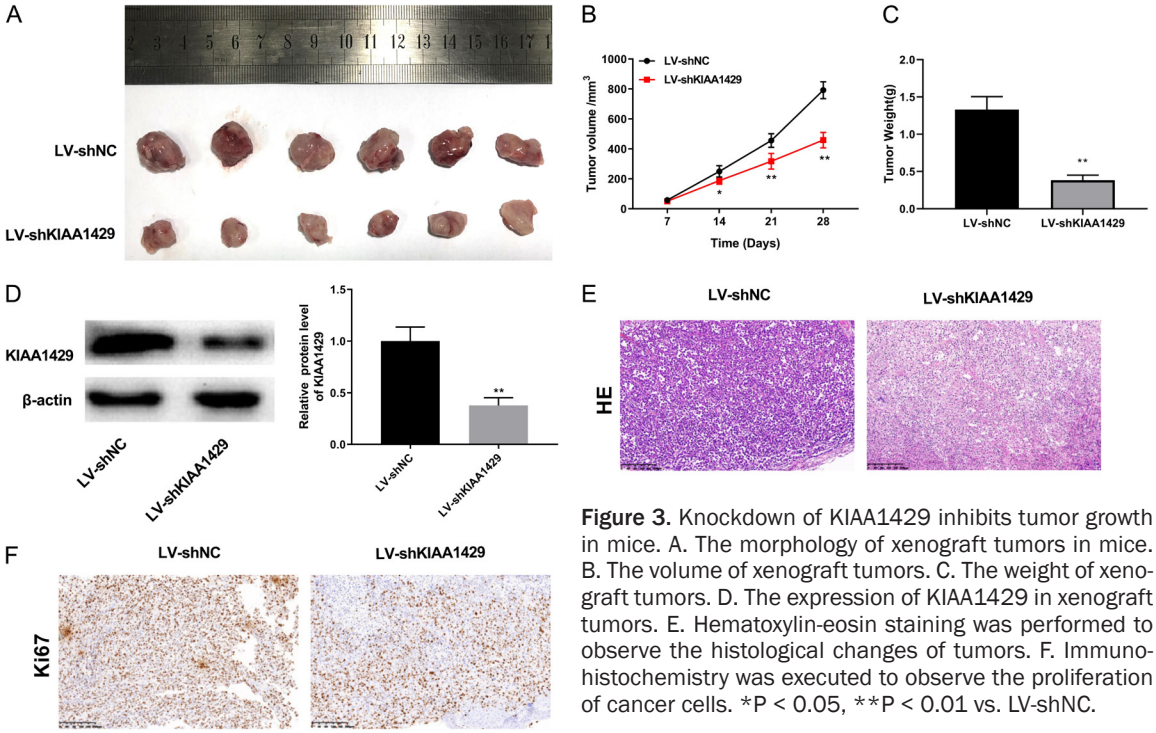

Figure 3. Knockdown of KIAA1429 inhibits tumor growth in mice. A. The morphology of xenograft tumors in mice. B. The volume of xenograft tumors. C. The weight of xenograft tumors. D. The expression of KIAA1429 in xenograft tumors. E. Hematoxylin-eosin staining was performed to observe the histological changes of tumors. F. Immunohistochemistry was executed to observe the proliferation of cancer cells. *P < 0.05, **P < 0.01 vs. LV-shNC.

with increasing erastin concentrations (**Figure 4A**). This inhibitory effect was reversed by adding the ferroptosis inhibitor Fer-1 (**Figure 4B**). Moreover, the knockdown of *KIAA1429* markedly increased the levels of ROS and Fe^{2+} and reduced those of GSH and MDA in the erastin-treated cells (**Figure 4C-F**). Additionally, erastin treatment markedly increased the protein expression of PTGS2 in the si-NC group and decreased that of GPX4 and FTH1 (**Figure 4G**, **4H**), similar to the si-KIAA1429 group. In summary, *KIAA1429* knockdown promoted erastin-mediated ferroptosis.

Transcriptome sequencing analysis

The molecular mechanisms downstream of *KIAA1429* silencing were explored in NSCLC cells. In total, 346 DEGs were identified, 196 of which were upregulated and 150 were downregulated (**Figure 5A** and **5B**). GO enrichment analysis revealed that the DEGs were enriched in various biological functions, including autolysosome, negative regulation of endoplasmic reticulum unfolded protein response, and secondary lysosome (rich > 0.2) (**Figure 6A**). Moreover, KEGG analysis showed that the DEGs were enriched in many pathways, including those related to galactose metabolism, mineral absorption, nicotine addiction, p53 signaling, and ferroptosis (**Figure 6B**).

Knockdown of KIAA1429 activates the p53 signaling pathway to inhibit NSCLC progression

The mechanism through which KIAA1429 regulates the p53 signaling pathway was further analyzed using H1299 cells. The western blot results revealed that the p-p53/p53 level was higher in the si-KIAA1429-transfected cells than in their si-NC-transfected counterparts (P < 0.01; **Figure 7A**). The p53 inhibitor PFT blocked the p53 signaling pathway by decreasing p-p53/p53 expression, whereas si-KIAA1429 reversed this effect (**Figure 7B**). Furthermore, functional assays showed that PFT

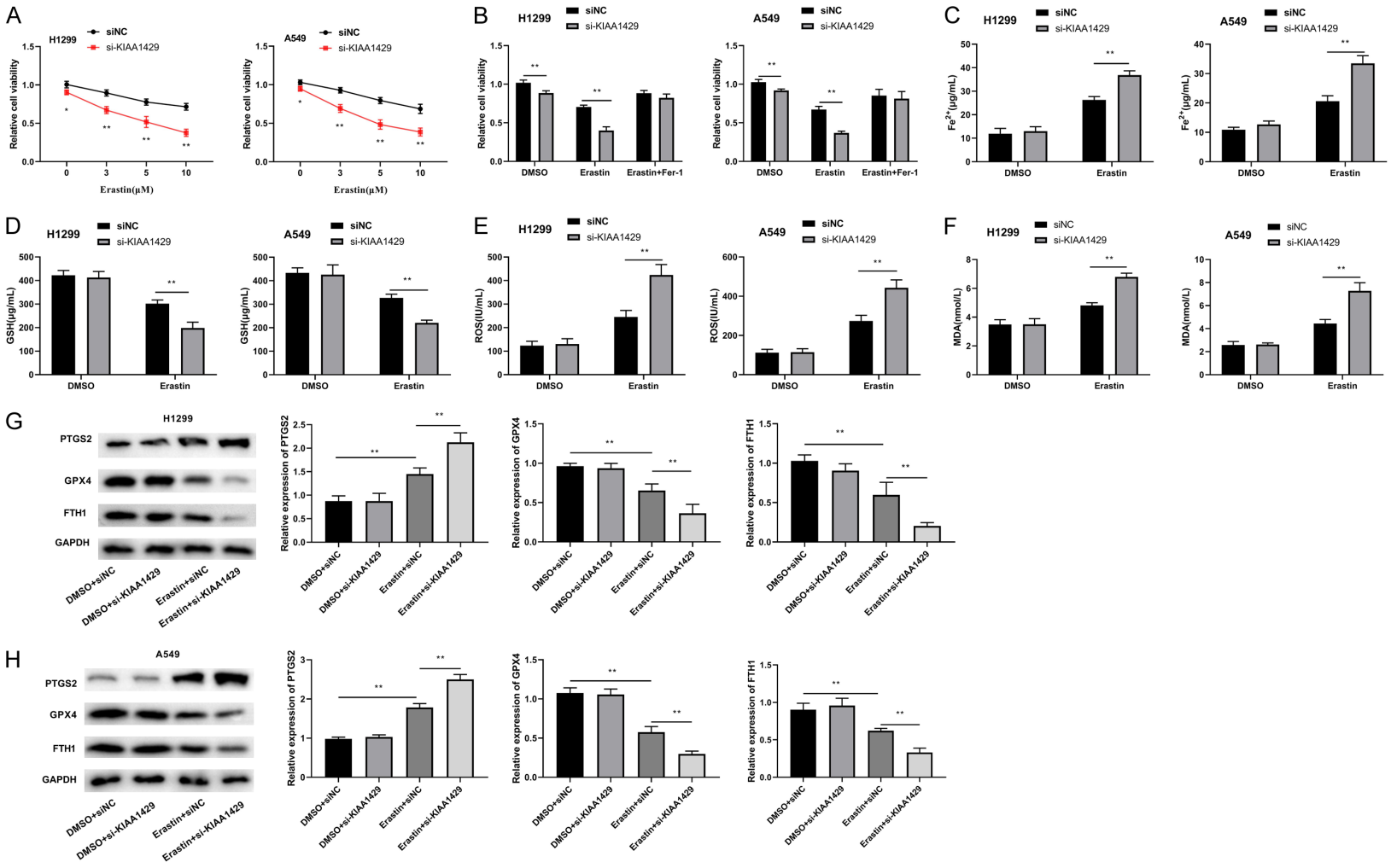

Figure 4. Knockdown of KIAA1429 promoted the ferroptosis in NSCLC cells. A. CCK-8 was executed to evaluate cell viability in A549 cells after erastin treatment. B. CCK-8 was executed to evaluate cell viability in H1299 and A549 cells after erastin (10 μM) ± ferrostatin-1 (2 μM). C-F. The levels of Fe^{2+} and lipid peroxidation indexes ROS, GSH and MDA in H1299 and A549 cells were detected by ELISA. G, H. Western-blot was used to detect the expression levels of ferroptosis-related proteins (PTGS2, GPX4, and FTH1) in H1299 and A549 cells. **P < 0.01 vs. si-NC.

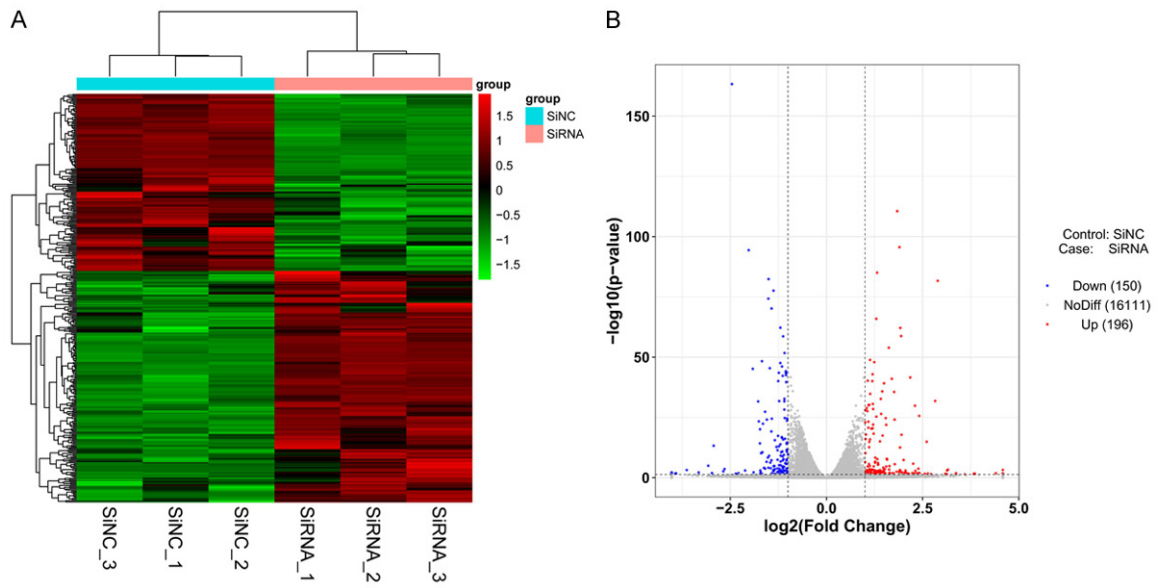

Figure 5. Differentially expressed genes (DEGs) in KIAA1429-silenced H1299 cells. A. A heatmap of DEGs in different groups. B. A Volcano map of DEGs.

significantly promoted the proliferative, migratory, and invasive abilities of the NSCLC cells relative to its effects on the si-NC group ($P < 0.01$, **Figure 7C-F**). Additionally, PFT weakened the inhibitory effects of si-KIAA1429 on NSCLC cell proliferation, migration, and invasion ($P < 0.01$, **Figure 7C-F**).

Discussion

NSCLC remains a leading cause of death worldwide, and effective treatments for improving the poor outcomes of affected patients remain a challenge [30]. Several lines of evidence have shown that the m^{6}A modification can influence diverse tumor characteristics, including the maintenance of proliferation signals, evasion of growth inhibition, resistance to apoptosis, induction of angiogenesis, activation of metastasis, changes in energy metabolism, and immune escape [31, 32]. KIAA1429 is the largest of the methyltransferases involved in m^{6}A modification [15]. KIAA1429 has multiple roles in various tumors. For example, *KIAA1429* silencing suppresses the proliferation and metastasis of hepatocellular carcinoma cells through the post-transcriptional regulation of GATA3 in an m^{6}A-dependent manner [12]. Furthermore, KIAA1429 enhances breast cancer progression by regulating CDK1 in an m^{6}A-independent manner [13]. Additionally, Xu et al. found that KIAA1429 enhanced the proliferation of NSCLC cells and the growth of NSCLC xenografts via the m^{6}A-dependent degradation of *DAPK3* mRNA [17]. In this study, we determined through public database analysis that KIAA1429 expression was upregulated in NSCLC tissues, and its high level correlated positively with poor overall survival. Our *in vitro* experiments verified that KIAA1429 was upregulated in NSCLC cells and that its knockdown inhibited malignant features at the cellular level. These results were similar to those of previous studies illustrating that *KIAA1429* acts as an oncogene in NSCLC. Furthermore, our *in vivo* experiments verified that *KIAA1429* silencing can inhibit the growth of tumor xenografts.

To identify the mechanisms of action downstream of KIAA1429 in NSCLC, transcriptome sequencing was performed on *KIAA1429*-silenced cells. Ferroptosis was selected as the research target, as it was enriched in the identified DEGs. *KIAA1429* silencing enhanced ferroptosis in the NSCLC cells, as evidenced by the increased Fe^{2+} and ROS and decreased GSH and MDA levels, as well as the upregulation of PTGS2 and downregulation of GPX4 and FTH1 expression. Ferroptosis is an iron-dependent cell death process that acts as a natural barrier to prevent the tumorigenesis, progression, and metastasis of diverse types of cancer [33]. Under oxidative stress conditions,

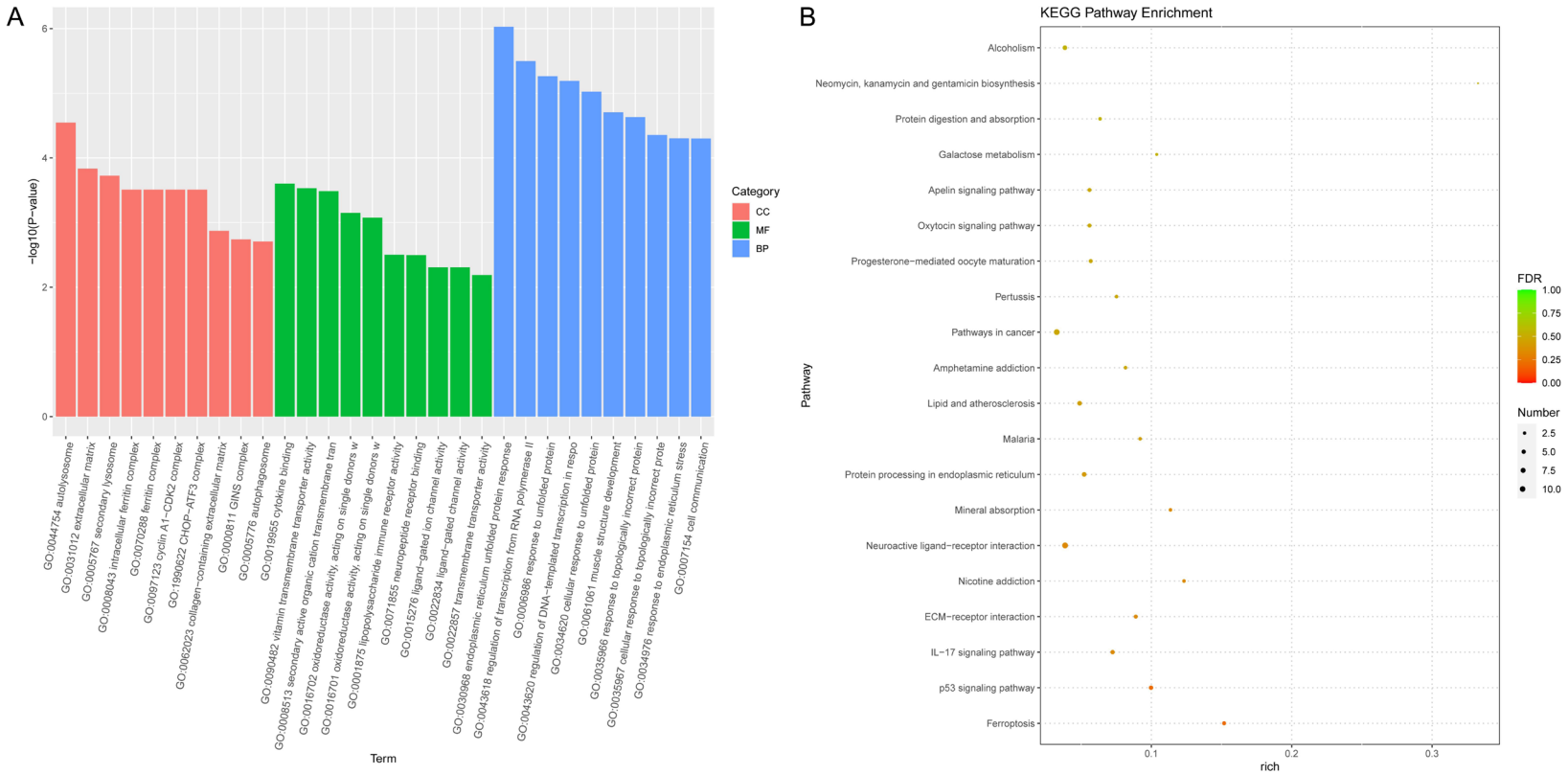

Figure 6. Functional enrichment of differentially expressed genes isolated from KIAA1429-silenced H1299 cells. A. Bar plot of GO enrichment analysis. B. Bubble plots of KEGG enrichment analysis.

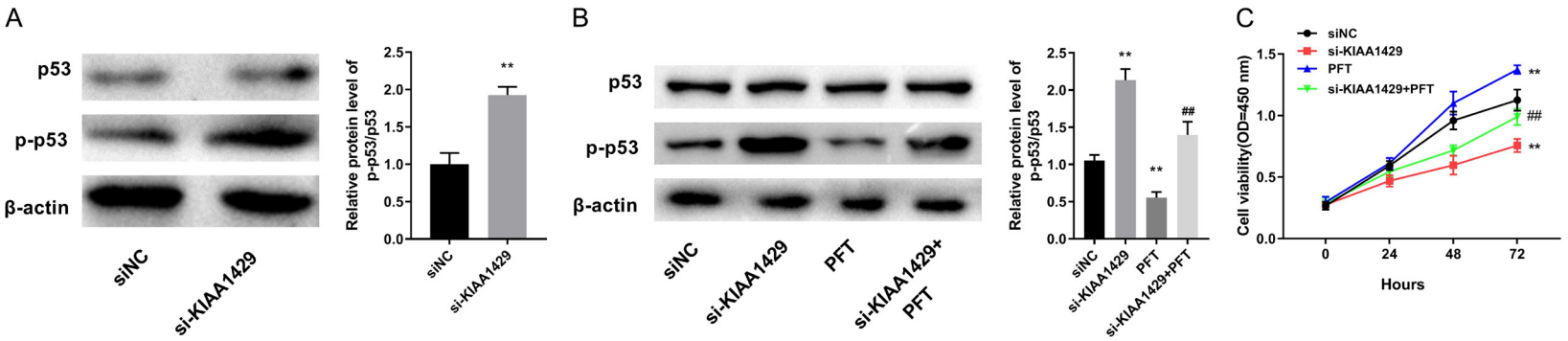

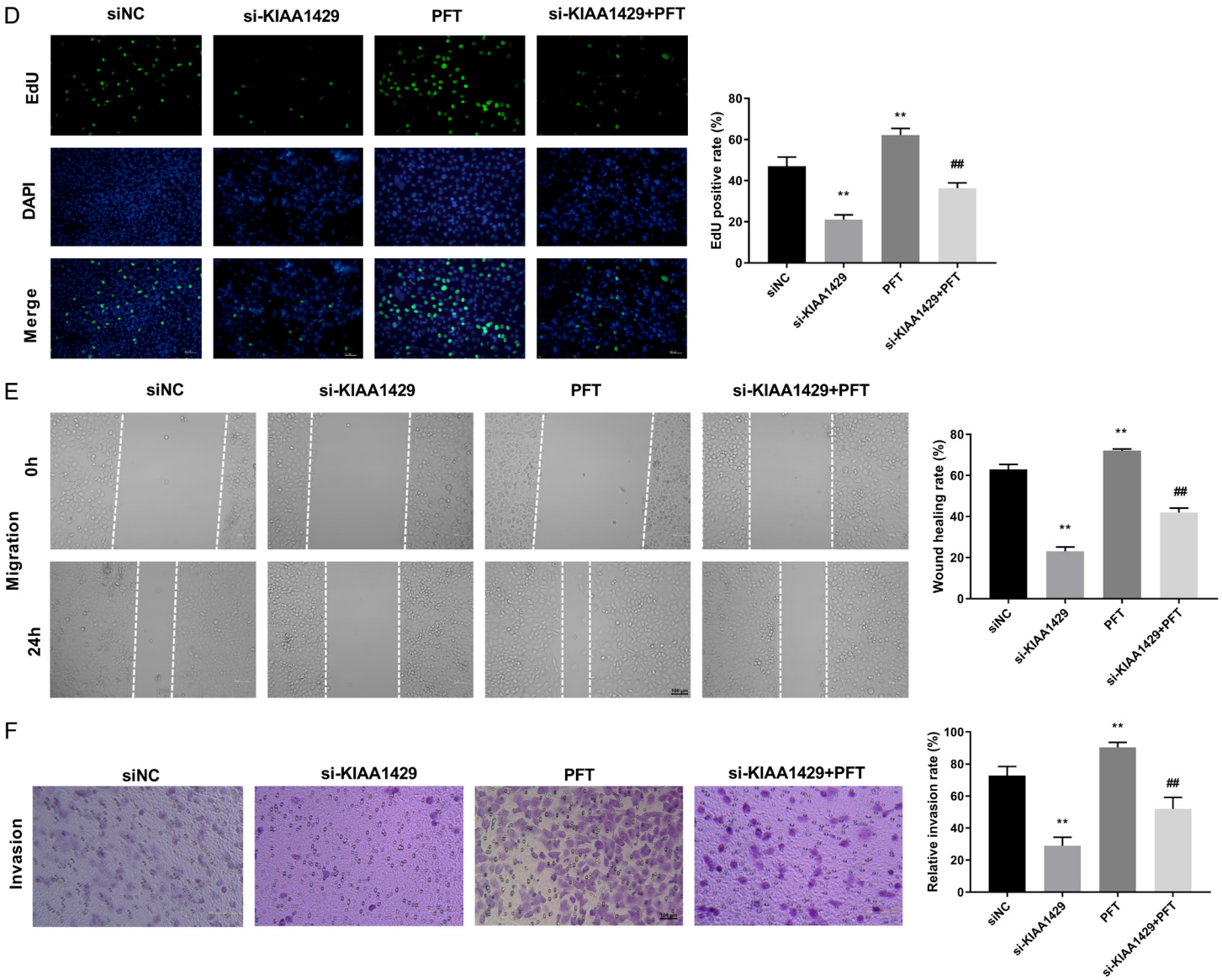

Figure 7. Knockdown of KIAA1429 activated the p53 signaling pathway to inhibit NSCLC progression. A. The expression of the p53 pathway-related proteins in H1299 cells was detected by Western blot. B. After PFT treatment, the expression of the p53 pathway-related proteins was detected by Western blot. C. The viability of transfected/treated H1299 cells was measured by CCK8 assay. D. EdU positive cells was detected by EdU assay (200×). E. The migration of transfected/treated H1299 cells was measured by wound healing assay. F. The invasion of transfected/treated H1299 cells was measured by Transwell assay (200×). **P < 0.01 vs. siNC; ##P < 0.01 vs. si-KIAA1429.

the ferroptosis defense system benefits the survival of tumor cells and their response to various cancer therapies [34]. Huang et al. found that the ferroptosis activator erastin inhibited the proliferation of lung cancer cells by arresting the cell cycle at the G1 phase [35]. Similarly, Chen et al. revealed that erastin suppressed the proliferative and migratory abilities of lung cancer cells by inducing calcium/calmodulin-dependent ferroptosis [36]. Other studies have determined the regulatory role of m^{6}A modification in ferroptosis [25-27]. Combined with the reverse regulatory relationship between KIAA1429 and ferroptosis, we speculate that activating this cell death process by silencing KIAA1429 may inhibit the progression of NSCLC.

In this study, the DEGs in *KIAA1429*-silenced NSCLC cells were also enriched in the p53 signaling pathway. p53 is an important tumor suppressor that inhibits cancer progression by regulating cell proliferation, apoptosis, and cell-cycle arrest [37]. Molecules such as TNFAIP8 [38], USP22 [39], HAX1 [40], and GINS2 [41] regulate the p53 signaling pathway and, thus, show therapeutic potential against NSCLC. Sang et al. reported that the m^{6}A methyltransferase subunits METTL3 and METTL14 enhanced acute myeloid leukemia by targeting the MDM2/p53 signaling pathway [42]. In our study, *KIAA1429* silencing promoted antitumor effects by facilitating the activation of the p53 signaling pathway, whereas PFT (a p53 inhibitor) reversed these effects of si-KIAA1429. These results indicate that the p53 signaling pathway is an active target of KIAA1429 and contributes to the remission of NSCLC. Moreover, p53 also plays a key regulatory role in ferroptosis [28, 29]. Huang et al. found that erastin-induced ROS production enhanced ferroptosis and inhibited cell proliferation by activating p53 in lung cancer cells [35]. Meng et al. showed that levobupivacaine inhibited ferroptosis in NSCLC and the progression of the disease by activating p53 [43]. In our study, *KIAA1429* silencing promoted erastin-induced ferroptosis and activated the p53 signaling pathway, revealing the potential mechanisms underlying the pathology of NSCLC.

Conclusions

In summary, the expression of the m^{6}A methyltransferase KIAA1429 was elevated in NSCLC tissues and cells. *KIAA1429* silencing promoted the p53 signaling pathway and ferroptosis in the NSCLC cells and inhibited their proliferative, migratory, and invasive abilities. *KIAA1429* silencing also inhibited the growth of tumor xenografts in mice. However, a limitation of our study is that it lacked human clinical samples for analysis; these should be considered in future studies. Nonetheless, our findings that KIAA1429 regulates the p53 signaling pathway and ferroptosis suggest that this m^{6}A methyltransferase can be a promising molecular target for treatment strategies against NSCLC.

Disclosure of conflict of interest

None.

Address correspondence to: Dr. Qunqing Chen, Department of Thoracic Surgery, Zhujiang Hospital, Southern Medical University, No. 253, Gongye Avenue, Guangzhou 510280, Guangdong, China. Tel: +86-13826038939; E-mail: chenqqg1985@163.com

References

[1] Relli V, Trerotola M, Guerra E and Alberti S. Abandoning the notion of non-small cell lung cancer. Trends Mol Med 2019; 25: 585-594.
[2] Duma N, Santana-Davila R and Molina JR. Non-small cell lung cancer: epidemiology, screening, diagnosis, and treatment. Mayo Clin Proc 2019; 94: 1623-1640.
[3] Uprety D, Mandrekar SJ, Wigle D, Roden AC and Adjei AA. Neoadjuvant immunotherapy for NSCLC: current concepts and future approaches. J Thorac Oncol 2020; 15: 1281-1297.
[4] Murugesan S, Murugesan J, Palaniappan S, Palaniappan S, Murugan T, Siddiqui SS and Loganathan S. Tyrosine kinase inhibitors (TKIs) in lung cancer treatment: a comprehensive analysis. Curr Cancer Drug Targets 2021; 21: 55-69.
[5] Herbst RS, Morgensztern D and Boshoff C. The biology and management of non-small cell lung cancer. Nature 2018; 553: 446-454.
[6] Imyanitov EN, Iyevleva AG and Levchenko EV. Molecular testing and targeted therapy for non-small cell lung cancer: current status and perspectives. Crit Rev Oncol Hematol 2021; 157: 103194.
[7] Jonna S and Subramaniam DS. Molecular diagnostics and targeted therapies in non-small cell lung cancer (NSCLC): an update. Discov Med 2019; 27: 167-170.
[8] Pian C, Yang Z, Yang Y, Zhang L and Chen Y. Identifying RNA N6-methyladenine sites in

three species based on a markov model. Front Genet 2021; 12: 650803.
[9] Zhong H, Tang HF and Kai Y. N6-methyladenine RNA modification (m(6)A): an emerging regulator of metabolic diseases. Curr Drug Targets 2020; 21: 1056-1067.
[10] Yang J, Chen J, Fei X, Wang X and Wang K. N6-methyladenine RNA modification and cancer. Oncol Lett 2020; 20; 1504-1512.
[11] Qiu FS, He JQ, Zhong YS, Guo MY and Yu CH. Implications of m6A methylation and microbiota interaction in non-small cell lung cancer: from basics to therapeutics. Front Cell Infect Microbiol 2022; 12: 972655.
[12] Lan T, Li H, Zhang D, Xu L, Liu H, Hao X, Yan X, Liao H, Chen X, Xie K, Li J, Liao M, Huang J, Yuan K, Zeng Y and Wu H. KIAA1429 contributes to liver cancer progression through N6-methyladenosine-dependent post-transcriptional modification of GATA3. Mol Cancer 2019; 18: 186.
[13] Qian JY, Gao J, Sun X, Cao MD, Shi L, Xia TS, Zhou WB, Wang S, Ding Q and Wei JF. KIAA1429 acts as an oncogenic factor in breast cancer by regulating CDK1 in an N6-methyladenosine-independent manner. Oncogene 2019; 38: 6123-6141.
[14] Miao R, Dai CC, Mei L, Xu J, Sun SW, Xing YL, Wu LS, Wang MH and Wei JF. KIAA1429 regulates cell proliferation by targeting c-Jun messenger RNA directly in gastric cancer. J Cell Physiol 2020; 235: 7420-7432.
[15] Ma L, Lin Y, Sun SW, Xu J, Yu T, Chen WL, Zhang LH, Guo YC, Wang YW, Chen T, Wei JF and Zhu LJ. KIAA1429 is a potential prognostic marker in colorectal cancer by promoting the proliferation via downregulating WEE1 expression in an m6A-independent manner. Oncogene 2022; 41: 692-703.
[16] Tang J, Han T, Tong W, Zhao J and Wang W. N(6)-methyladenosine (m(6)A) methyltransferase KIAA1429 accelerates the gefitinib resistance of non-small-cell lung cancer. Cell Death Discov 2021; 7: 108.
[17] Xu Y, Chen Y, Yao Y, Xie H, Lu G, Du C, Cheng J and Zhou J. VIRMA contributes to non-small cell lung cancer progression via N(6)-methyladenosine-dependent DAPK3 post-transcriptional modification. Cancer Lett 2021; 522: 142-154.
[18] Li J, Cao F, Yin HL, Huang ZJ, Lin ZT, Mao N, Sun B and Wang G. Ferroptosis: past, present and future. Cell Death Dis 2020; 11: 88.
[19] Wei X, Yi X, Zhu XH and Jiang DS. Posttranslational modifications in ferroptosis. Oxid Med Cell Longev 2020; 2020: 8832043.
[20] Lu X, Kang N, Ling X, Pan M, Du W and Gao S. MiR-27a-3p promotes non-small cell lung cancer through SLC7A11-mediated-ferroptosis. Front Oncol 2021; 11: 759346.
[21] Gai C, Liu C, Wu X, Yu M, Zheng J, Zhang W, Lv S and Li W. MT1DP loaded by folate-modified liposomes sensitizes erastin-induced ferroptosis via regulating miR-365a-3p/NRF2 axis in non-small cell lung cancer cells. Cell Death Dis 2020; 11: 751.
[22] Huang F, Zheng Y, Li X, Luo H and Luo L. Ferroptosis-related gene AKR1C1 predicts the prognosis of non-small cell lung cancer. Cancer Cell Int 2021; 21: 567.
[23] Wei D, Ke YQ, Duan P, Zhou L, Wang CY and Cao P. MicroRNA-302a-3p induces ferroptosis of non-small cell lung cancer cells via targeting ferroportin. Free Radic Res 2021; 55: 821-830.
[24] Shanshan W, Hongying M, Jingjing F, Yiming Y, Yu R and Rui Y. CircDTL functions as an oncogene and regulates both apoptosis and ferroptosis in non-small cell lung cancer cells. Front Genet 2021; 12: 743505.
[25] Shen M, Li Y, Wang Y, Shao J, Zhang F, Yin G, Chen A, Zhang Z and Zheng S. N(6)-methyladenosine modification regulates ferroptosis through autophagy signaling pathway in hepatic stellate cells. Redox Biol 2021; 47: 102151.
[26] Liu L, He J, Sun G, Huang N, Bian Z, Xu C, Zhang Y, Cui Z, Xu W, Sun F, Zhuang C, Man Q and Gu S. The N6-methyladenosine modification enhances ferroptosis resistance through inhibiting SLC7A11 mRNA deadenylation in hepatoblastoma. Clin Transl Med 2022; 12: e778.
[27] Song Z, Jia G, Ma P and Cang S. Exosomal miR-4443 promotes cisplatin resistance in non-small cell lung carcinoma by regulating FSP1 m6A modification-mediated ferroptosis. Life Sci 2021; 276: 119399.
[28] Liu J, Zhang C, Wang J, Hu W and Feng Z. The regulation of ferroptosis by tumor suppressor p53 and its pathway. Int J Mol Sci 2020; 21: 8387.
[29] Huang CL, Yokomise H and Miyatake A. Clinical significance of the p53 pathway and associated gene therapy in non-small cell lung cancers. Future Oncol 2007; 3: 83-93.
[30] Gridelli C, Rossi A, Carbone DP, Guarize J, Karachaliou N, Mok T, Petrella F, Spaggiari L and Rosell R. Non-small-cell lung cancer. Nat Rev Dis Primers 2015; 1: 15009.
[31] Liu L, Li H, Hu D, Wang Y, Shao W, Zhong J, Yang S, Liu J and Zhang J. Insights into N6-methyladenosine and programmed cell death in cancer. Mol Cancer 2022; 21: 32.
[32] Li Y, Gu J, Xu F, Zhu Q, Chen Y, Ge D and Lu C. Molecular characterization, biological function, tumor microenvironment association and

clinical significance of m6A regulators in lung adenocarcinoma. Brief Bioinform 2021; 22: bbaa225.
[33] Liu X, Zhang Y, Wu X, Xu F, Ma H, Wu M and Xia Y. Targeting ferroptosis pathway to combat therapy resistance and metastasis of cancer. Front Pharmacol 2022; 13: 909821.
[34] Lei G, Zhuang L and Gan B. Targeting ferroptosis as a vulnerability in cancer. Nat Rev Cancer 2022; 22: 381-396.
[35] Huang C, Yang M, Deng J, Li P, Su W and Jiang R. Upregulation and activation of p53 by erastin-induced reactive oxygen species contribute to cytotoxic and cytostatic effects in A549 lung cancer cells. Oncol Rep 2018; 40: 2363-2370.
[36] Chen P, Wu Q, Feng J, Yan L, Sun Y, Liu S, Xiang Y, Zhang M, Pan T, Chen X, Duan T, Zhai L, Zhai B, Wang W, Zhang R, Chen B, Han X, Li Y, Chen L, Liu Y, Huang X, Jin T, Zhang W, Luo H, Chen X, Li Y, Li Q, Li G, Zhang Q, Zhuo L, Yang Z, Tang H, Xie T, Ouyang X and Sui X. Erianin, a novel dibenzyl compound in dendrobium extract, inhibits lung cancer cell growth and migration via calcium/calmodulin-dependent ferroptosis. Signal Transduct Target Ther 2020; 5: 51.
[37] Chiang YT, Chien YC, Lin YH, Wu HH, Lee DF and Yu YL. The function of the mutant p53-R175H in cancer. Cancers (Basel) 2021; 13: 4088.
[38] Xing Y, Liu Y, Liu T, Meng Q, Lu H, Liu W, Hu J, Li C, Cao M, Yan S, Huang J, Wang T and Cai L. TNFAIP8 promotes the proliferation and cisplatin chemoresistance of non-small cell lung cancer through MDM2/p53 pathway. Cell Commun Signal 2018; 16: 43.
[39] Ding F, Bao C, Tian Y, Xiao H, Wang M, Xie X, Hu F and Mei J. USP22 promotes NSCLC tumorigenesis via MDMX up-regulation and subsequent p53 inhibition. Int J Mol Sci 2014; 16: 307-20.
[40] Liang Z, Zhong Y, Meng L, Chen Y, Liu Y, Wu A, Li X and Wang M. HAX1 enhances the survival and metastasis of non-small cell lung cancer through the AKT/mTOR and MDM2/p53 signaling pathway. Thorac Cancer 2020; 11: 3155-3167.
[41] Chi F, Wang Z, Li Y and Chang N. Knockdown of GINS2 inhibits proliferation and promotes apoptosis through the p53/GADD45A pathway in non-small-cell lung cancer. Biosci Rep 2020; 40: BSR20193949.
[42] Sang L, Wu X, Yan T, Naren D, Liu X, Zheng X, Zhang N, Wang H, Li Y and Gong Y. The m(6)A RNA methyltransferase METTL3/METTL14 promotes leukemogenesis through the mdm2/p53 pathway in acute myeloid leukemia. J Cancer 2022; 13: 1019-1030.
[43] Meng M, Huang M, Liu C, Wang J, Ren W, Cui S, Gu J, Xie J, Ma B, Yang G and He S. Local anesthetic levobupivacaine induces ferroptosis and inhibits progression by up-regulating p53 in non-small cell lung cancer. Aging (Albany NY) 2021; [Epub ahead of print].

Table S1. siRNA sequences in this study

siRNA	Sequences (5'-3')
siNC-sense	UUC UCC GAA CGU GUC ACG UTT
siNC-antisense	ACG UGA CAC GUU CGG AGA ATT
siKIAA1429-1-sense	CCAUCAUCUUUAGACCUAATT
siKIAA1429-1-antisense	UUAGGUCUAAAGAUGAUGGTT
siKIAA1429-2-sense	GCUCAAAGCUGGGACCAAATT
siKIAA1429-2-antisense	UUUGGUCCCAGCUUUGAGCTT
siKIAA1429-3-sense	GGAGUUGGUUACCUUGCUUTT
siKIAA1429-3-antisense	AAGCAAGGUAACCAACUCCTT

Table S2. Primer sequences for qRT-PCR in this study

Primer	Sequences (5'-3')
GAPDH-F	CCGGGAAACTGTGGCGTGATGG
GAPDH-R	AGGTGGAGGAGTGGGTGTCGCTGTT
KIAA1429-F	CACGACACAGATGCTGGACT
KIAA1429-R	TTGTATGAGGGGCAGTTTCC